

## MAGNETIC RECONNECTION IN THE ABSENCE OF THREE-DIMENSION NULL POINT

Ali K.H. Al-Hachami

alhachamia@uowasit.edu.iq

University of Wassit, College of Education for Pure Science, Al Kūt, Wasit, Iraq

---

### Abstract

In this study, a numerical examination is portrayed which explores the idea of 3D reconnection, in the absence of magnetic null points focuses, at a segregated non-ideal region. We center around the subsequent conduct of the magnetic flux, which has been appeared D.I. Pontin<sup>1</sup> et al. (2004), to be on a very basic level diverse in the kinematic routine from the natural two-dimensional conduct. The point of this numerical investigation is to test whether the new properties of 3D kinematic reconnection, depicted by D.I. Pontin et al. (2004) finish to the dynamical routine, where magnetohydrodynamics equations are unraveled. We point likewise specifically to check (or something else) the arrangement by G. Hornig and E.R. Priest (2003) for kinematic 3D reconnection without an magnetic null point

### Keywords

*Magnetohydrodynamics (MHD), magnetic reconnection, Sun, corona — Sun, magnetic topology*

Received 09.09.2019

© Author(s), 2019

---

**Introduction.** The manner by which magnetic field lines break and reconnect in two dimensions is currently genuinely surely known, albeit a few inquiries regarding the subtleties remain [1–3]. A two-dimensional magnetic setup might be split up into topological particular districts by separatrices, which are uncommon field lines that by and large cross at X-type neutral points. Three-dimensional parts of reconnection are profoundly perplexing and are just barely starting to be comprehended. When null points are present, it is regularly conceivable to sum up the two-dimensional picture in a straight-forward manner. The separatrix curves become separatrix surfaces which split the volume into topologically distinct regions, as in a specific district contains just field lines which begin at one specific source and end up at another specific

---

<sup>1</sup> Pontin D.I., Hornig G., Priest E.R. Kinematic reconnection at a magnetic null point: spine-aligned current. *Geophys. Astrophys. Fluid Dynamics*, 2004, vol. 98, iss. 5, pp. 407–428. DOI: <http://doi.org/10.1080/0309192042000272324>

source. The separatrices at that point meet in an extraordinary field line called a separator which closures at either three-dimensional neutral points or points on a boundary. This way of thinking has been followed in building the three-dimensional topology in solar flares [4, 5]) and in X-ray splendid focuses [6]. In such cases, coronal field lines with two endpoints on the photosphere produce a mapping from one piece of the photospheric surface to another. Such a mapping is, when all is said in done, piecewise ceaseless, and the separatrix surfaces separate the areas related with each persistent piece of the mapping (e.g., [7]). At the point when reconnection happens, magnetic flux is then moved over the separatrices starting with one area then onto the next. The importance of a piece of  $E$  parallel to  $B$  in reconnection has been depicted by, for example Ref. [8, 9]. The activity of this parallel electric field in our assessment is depicted in detail.

There are currently a lot of 3D numerical analyses into different utilizations of reconnection. Of those 3D MHD recreations which are expected to concentrate on the reconnection procedure itself, there are various investigations of the connection of separated magnetic flux tubes in different diverse 3D designs (for example Ref. [10–12]). Reenactments have additionally been made of 3D reconnection in magnetic fields containing invalid focuses (for example Ref. [13, 14]) just as when no invalid focuses are available (e.g., Ref. [13, 15] and Ref. [16]), where as a rule a great deal of the emphasis has been on deciding at which areas flows specially develop. In the test depicted in this study, we consider such an arrangement where the current is known to develop, and spotlight on the conduct of the magnetic flux when a resistivity is acquainted with encourage reconnection.

In Section *Numerical plan* we portray the numerical plan, just as the underlying setup and boundary conditions. In Section *Result* the consequences of the examination a spoke to for reconnection at a fixed disconnected diffusion region.

**Numerical plan.** So as to play out the investigation we utilize a parallel numerical code to solve the dimensionless equation of MHD in the structure:

$$\begin{aligned}\frac{\partial \mathbf{B}}{\partial t} &= -\nabla \times \mathbf{E}; \\ E &= -(\mathbf{v} \times \mathbf{B}) + \eta \mathbf{J}; \\ \nabla \times \mathbf{B} &= \mathbf{J}; \\ \frac{\partial \rho}{\partial t} &= -\nabla \cdot (\rho \mathbf{v}); \\ \frac{\partial}{\partial t} (\rho \mathbf{v}) &= -\nabla \cdot (\rho \mathbf{v} \mathbf{v} + \boldsymbol{\tau}) - \nabla P + \mathbf{j} \times \mathbf{B};\end{aligned}$$

$$\frac{\partial e}{\partial t} = -\nabla \cdot (e\mathbf{v} + \boldsymbol{\tau}) - \nabla P \cdot \mathbf{v} + Q_{visc} + Q_{joule},$$

where  $\mathbf{B}$  is the magnetic field,  $\mathbf{E}$  the electric field,  $\mathbf{v}$  is the plasma velocity,  $\eta$  is the resistivity,  $\mathbf{J}$  is the electric current,  $\rho$  is the density,  $\boldsymbol{\tau}$  is the viscous stress tensor,  $P$  is the pressure,  $e$  is the internal energy,  $Q_{visc}$  is the viscous dissipation,  $Q_{joule}$  is the Joule dissipation.

Note that the equations above have been non-dimensionalized by setting the magnetic porousness  $\mu_0 = 1$ , and the gas consistent equivalent to the mean sub-atomic weight. The outcome is that, for a cubic area of unit estimate (as depicted in the accompanying analysis), if  $|\rho|$  and  $|B|=1$ , at that point the time is estimated in units of the Alfvén travel time across the space ( $\tau_A = L\sqrt{\mu_0\rho_0}$ , where  $L$  is the extent of the domain,  $\rho_0$  and  $B_0$  are typical values of the density and magnetic field respectively).

We perform two arrangements of keeps running of the investigation; in the first we accept the *cold plasma* approximation, that the thickness and inside vitality are steady. Various runs are performed of various numerical resolution, with the equations comprehended on Cartesian grid of size,  $64^3$ ,  $128^3$  and  $256^3$ . The factors are assessed on stunned lattices; as for a unit 3D shape,  $\rho$  and  $e$  are determined in the body focus, and  $\mathbf{E}$  and  $\mathbf{j}$  are determined at face focuses,  $\mathbf{B}$  and  $\rho\mathbf{v}$  are determined at edge focuses. Spatial subsidiaries are assessed utilizing a 6th order accurate finite difference technique. This strategy includes the six closest neighbor focuses the pertinent way, and the equation for computing subsidiaries are gotten by basic change of the lists in the articulation below. The six administrators  $\partial^{\pm}_{,[xyz]}$  give an incentive for the derivative evaluated at  $\pm(1/2)$  grid point the significant way and, for instance,  $\partial^{\pm}_{,x}$  is given by

$$\begin{aligned} \partial^{\pm}_{,x}(f_{i,j,k}) &= f'_{i+1/2,j,k} = \\ &= \frac{a}{\Delta x}(f_{i,j,k} + f_{i+1,j,k}) + \frac{b}{\Delta x}(f_{i-1,j,k} + f_{i+2,j,k}) + \frac{c}{\Delta x}(f_{i-2,j,k} + f_{i+3,j,k}), \end{aligned}$$

where

$$a = 1 - 3b + 5c, \quad b = -\frac{1}{24} - 5c, \quad c = \frac{3}{640}.$$

Usually the case that, because of the amazed work, this estimation of the subsidiary is returned in precisely the position it is required. At the point when this isn't the situation, the qualities are introduced with a fifth-order

interpolation strategy utilizing one of six “shift” operators  $(T_{[xyz]}^\pm)$ , which insert the estimation of the picked capacity at matrix point the applicable way. For instance,  $T_x^+$  is given by

$$T_x^\pm(f_{i,j,k}) = f_{i+\frac{1}{2},j,k} = \\ = a(f_{i,j,k} + f_{i+1,j,k}) + b(f_{i-1,j,k} + f_{i+2,j,k}) + c(f_{i-2,j,k} + f_{i+3,j,k}),$$

where

$$a = \frac{1}{2} - b - c, \quad b = -\frac{1}{16} - 3c, \quad c = \frac{3}{256}.$$

For further clarification of the decision and execution of these administrators, see Ref. [17]. A third-order predictor-corrector strategy is utilized for time-venturing. It is a change of that by Hyman [18], adjusted to take into consideration variable time-venturing, and the indicator step is given by

$$f_{n+1}^* = a_1 f_{n-1} + (1 - a_1) f_n + b_1 \dot{f}_n,$$

while the corrector step is

$$f_{n+1} = a_2 f_{n-1} + (1 - a_2) f_n + b_2 \dot{f}_n + c_2 \dot{f}_{n+1}^*.$$

Here

$$a_1 = r^2, \quad b_1 = \Delta t_{n+1/2} (1 + r), \quad a_2 = 2(1 + r) / (2 + 3r),$$

$$b_2 = \Delta t_{n+1/2} (1 + r^2) / (2 + 3r),$$

$$c_2 = \Delta t_{n+1/2} (1 + r) / (2 + 3r), \quad r = \Delta t_{n+1/2} / \Delta t_{n-1/2}, \quad \Delta t_{n+1/2} = t_{n+1} - t_n$$

and  $\Delta t_{n-1/2} = t_n - t_{n-1}$ .

Data in regards to the execution of this plan in the code is given by Ref. [17]. In the code, counterfeit dissemination and consistency terms are incorporated which have been deliberately picked in order to give a restricted impact in circumstances where dissipative impacts are immaterial, yet which are additionally equipped for giving adequate confined scattering where important to deal with the improvement of numerical hazards. The decision of these terms depends on various tests for model circumstances, as portrayed by Ref. [17]. Furthermore, for various keeps running of the test, additional resistive terms are included.

*The experiment.* The point of the experiment is to think about the development of magnetic flux in are connection process including no invalid

purpose of  $\mathbf{B}$ , so as to test the attestations of Priest et al. [6] and Hornig and Priest [19]. They contemplated the straightforward magnetic field  $\mathbf{B} = B_0 (y/L, k^2x/L, 1)$ , where  $B_0, k$  and  $L$  are constant. It is in view of this that we pick our underlying magnetic field design to have the essential type of a hyperbolic X-type structure in one plane, with a unidirectional field the perpendicular direction. Such a field structure is named a *hyperbolic flux tube* (HFT), which by and large can be considered as the crossing point of two *semi separatrix layers* (QSLs).

So as to set up such an underlying magnetic field we pursue Galsgaard et al. [14] in ascertaining first the potential field coming about because of a magnetic field forced ordinary to two inverse limits. The  $x$ -part of the magnetic field is forced upon the two  $x$ -limits,  $x = \pm 0.5$ , and for each situation appears as two motion patches and a foundation field, with inverse extremity one each limit. The transition fixes each have uneven Gaussian profile, and are fixated on  $(x, y, z) = (-0.5, \pm y_0, 0)$  and  $(0.5, 0, \pm z_0)$ , where the numerical area keeps running from  $-0.5$  to  $0.5$  toward every path (see Fig. 1). Note that the setups

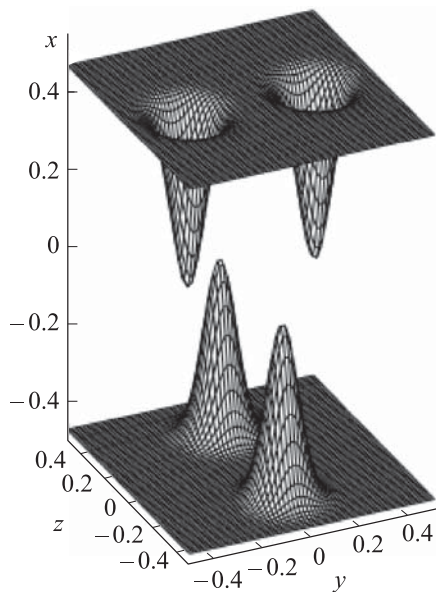


**Fig. 1.** The boundary conditions  $B_x$  on toward the beginning of the recreation. Two flux patches of inverse extremity are superimposed upon powerless foundation fields of inverse extremity on inverse  $x$ -boundaries

of the transition fixes on every limit are the equivalent; then again, actually the two are turned by  $90^\circ$  as for each other. The pinnacle quality of the magnetic field within the patches is  $0.5$ , while the foundation field is multiple times flimsier. The flux from these patches spreads out to fill the area, and at the focal plane of the space ( $x = 0$ ), the field is roughly uniform, and has a quality of  $\sim 0.072$ . In planes of consistent  $x$ , the field has a hyperbolic X-type structure.

It is imperative to take note of that, so as to accomplish this numerical setup, the limit conditions in the  $x$ - and  $y$ -direction are periodic. This implies, in spite of the fact that the underlying magnetic field is moderately straightforward, when the framework is aggravated and focused on auxiliary impacts will grow, for example, the development of current fixations, because of the collaboration of neigh-

boring frameworks. When all is said in done however, these impacts are commanded by those of the weight on the individual framework. Driven boundary conditions are connected on the  $x$ -boundary, as depicted beneath.

The driving speed on the limits is a shear movement, and is picked to be in the “twisting” sense, in order to shape a present layer along the focal pivot of the HFT, as depicted by Ref. [14]. The shear has a sinusoidal dependence, and is again unique on the two limits by a pivot of  $90^\circ$ . On every limit, it acts to advect the motion fixes in inverse ways opposite to the line that at first goes along with them (see Fig. 2). In particular, we force

$$v_{yz} = (x = -0.5) = (-v_0 \sin 2\pi z, 0), \quad v_{yz} = (x = 0.5) = (0, v_0 \sin 2\pi y),$$

where  $v_0$  ascends from zero over a period  $t$  to a consistent esteem, at which it stays for the remainder of the reproduction. The slow ascent is incorporated to limit the impact of Alfvén waves which engender into the space when the limit movement is started. These waves cause bothersome impacts, for example, a wavering of the field lines, which muddles the development of the magnetic flux that we plan to consider. They likewise make weak current focuses at their fronts. The time,  $t_0$ , over which the driving speed develops to its greatest esteem is picked to be 0.5, which is found to give a sensible decrease of these unwanted impacts, while further increment in is by all accounts of little assistance.

The plasma parameters for the recreation are as per the following. The thickness and warm vitality are both at first uniform, and take esteems 0.1 and 0.01 in our normalize units separately. This implies the sound speed ( $c_s = \sqrt{\gamma P / \rho}$ ) is uniform at 0.33, while the plasma beta ( $\beta = 2\mu P / B^2$ ) and Alfvén speed ( $v_A = |B| / \sqrt{\mu\rho}$ ) take estimations of around 2.57 and 0.23, individually, at the focal point of the area and 0.04 and 1.58, separately, at the focuses of the flux patches. Thus, the Alfvén crossing time is around 4 time units. The inevitable relentless incentive for the driving speed ( $v_0$ ) is 0.02, which is 13 of the neighborhood Alfvén speed in the district of foundation field and the Alfvén speed at the flux patches.

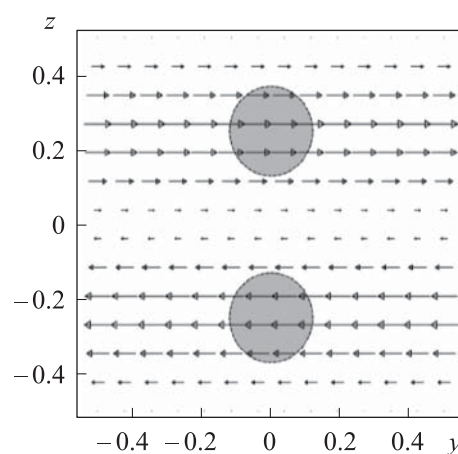


**Fig. 2.** The forced plasma velocity on the boundary  $x = -0.5$ ; the circles speak to the transition patches



At last, so as to accomplish our objective of researching the conduct of magnetic motion being reconnected at a confined non-ideal region, we force a resistivity ( $\eta$ ). We have made two classes of kept running with contrastingly endorsed resistivity. In the first (described in Section *Result*),  $\eta$  is forced to have a circularly symmetric exponential reliance of the form

$$\eta = \eta_0 e^{-(r/r_0)^2},$$

where  $\eta_0$  is chosen to be  $1 \cdot 10^{-3}$  and is chosen to be 0.06, so that non-ideal procedures are localized inside a little locale focused on the origin. In the second arrangement of runs,  $\eta$  is endorsed to rely upon the modulus of the current, so that  $\eta$  is a zero wherever that the current is beneath an edge esteem  $J_0$ , while in districts where  $|J|$  surpasses  $J_0$ ,  $\eta$  is given by

$$\eta = \eta_0 \sqrt{\frac{|J|^2 - J_0^2}{|J|^2}},$$

where  $\eta_0$  presently picked to be  $5 \cdot 10^{-4}$ , so that develops rapidly where increments above.

**The result.** We depict first the aftereffects of the keeps running with a fixed district of resistivity in the center of the domain. Runs were made exposed to the harsh elements' plasma limit at three different resolutions, on  $64^3$ ,  $128^3$  and  $256^3$ . Cartesian grids. Contrasts between the distinctive goals cold plasma runs are depicted as and when they happen in the following section. Every one of the analyses portrayed is kept running from time  $t = 0$  to  $t = 19$ .

*Electric current.* Toward the start of the simulation, the magnetic field is potential and the plasma is very still, thus there are no flows and no reconnection. As the recreation advances, and the boundary flux focuses are sheared, the QSLs of the field structure crease up from their underlying symmetrical setup. A related development of the current concentrations at the focal point of the domain because of the geometric structure of the magnetic field. The pinnacle current in the focal point of the area lies in the negative  $x$ -direction, against parallel to the magnetic field on the  $x$ -axis. Note, in any case, that the most extreme current inside the space before the finish of the run is quite the transition sources on the  $x$ -boundary, as there is no resistivity here to enable the current to disperse.

The development of  $|j|$  in the  $x = 0$  plane is appeared in Fig. 3. It develops roughly directly as time advances, despite the fact that there are normal changes from the straight development (Fig. 3, *a*). The reason for these changes is portrayed by Mellor et al. [20], who play out a comparable analysis. The current

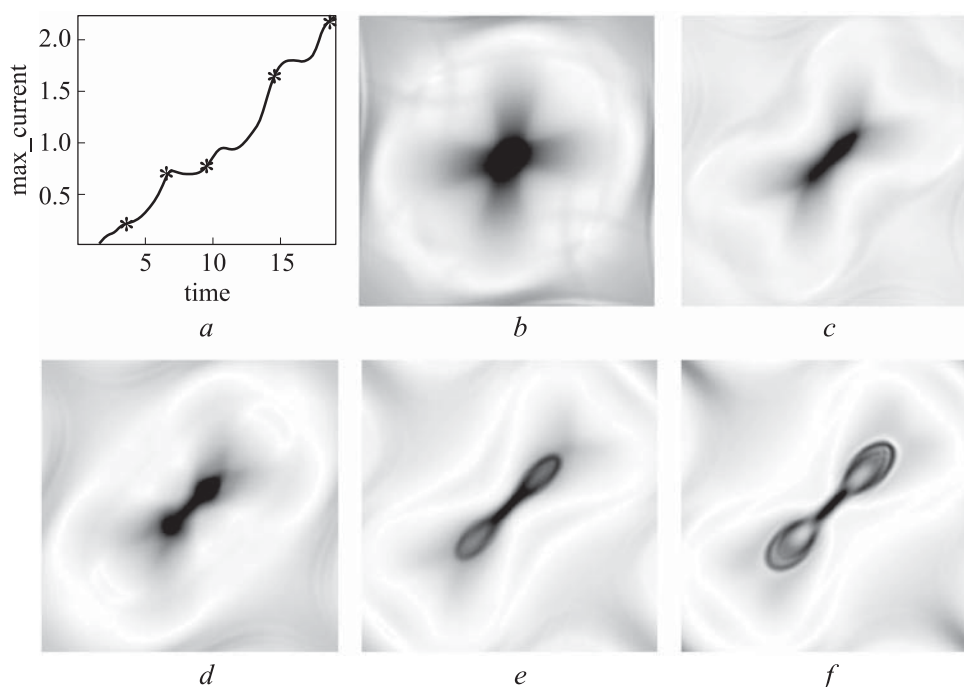


**Fig. 3.** (a) Growth of the maximum value of  $|j|$  in the  $x = 0$  plane, and (b–f) shaded scaled images showing  $|j|$  at intervals throughout the run (in each image the intensity is scaled to the maximum in that image, where white is zero current density and dark is high). The asterisks in (a) mark the times of the images (b–f)

basically increments in a stage like style because of the Alfvén waves set off by the boundary motion, which intermittently go through the focal plane, because of reflections off inverse limits. Here the damping procedure isn't as clear as in the explanatory model of Mellor, et al. [20], as the resistivity is just noteworthy in a little bit of the area. One contrast between the keeps running of various goals is that the pinnacle current in the focal plane is really higher in keeps running of lower goals, by a factor of around 30 for each adjustment in goals. This is presumably on the grounds that the dissemination is nearer to appropriately settled in the higher goals keeps running since there are more grid point focuses inside the successful non-ideal locale.

Figures 3, b–f demonstrates the advancement of the current focus in the focal plane, where the shading in strained quality is standardized to the most extreme incentive in every individual casing. These most extreme qualities can be seen from the diagram in Fig. 3 a, where the information focuses comparing to the seasons of the Fig. 3, b–f are set apart with reference marks. The present fixation step by step crumples towards the  $y = z$  line, from an underlying inexact hover shape, as the field turns out to be increasingly bent. This present focus stays all



around settled all through the reenactment, since the resistivity inevitably acts to stop the breakdown, by enabling the current to diffuse outwards (from the X-line, where X-line will hereafter be utilized to allude to the  $x$ -axis, along which  $B_{yz}$  has a X-point structure). It is conceivable to make certain that the current fixation stays very much settled since its width remains roughly consistent for keeps running of various goals, and is around 16 matrix focuses (full-width at half-most extreme) in the  $256^3$  run.

*Plasma flow.* Despite the fact that a shear plasma stream is forced upon the  $x$ -boundary of the area, the stream inside the volume isn't forced, thus advances unreservedly, in spite of the fact that it is obviously impacted by the limit move-

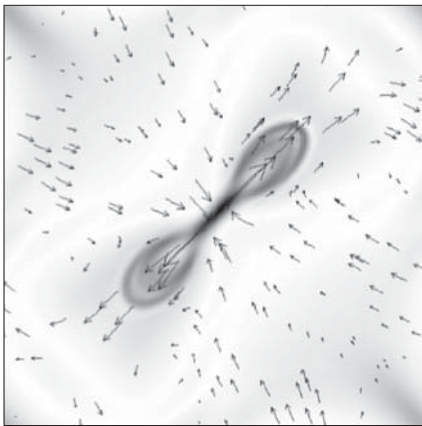


**Fig. 4.** The plasma velocity in the  $x = 0$  plane at  $t = 19$  (the end of the run). The vectors indicate the strength and direction of  $v_{yz}$ , while the background is shaded to show  $|j|$

ment. Analyzing by and by the  $x = 0$  plane, in which the magnetic field has a hyperbolic structure, we find that the plasma stream builds up a stagnation-point structure, as appeared in Fig. 4. The foundation shading in the picture demonstrates the modulus of the current in a similar plane. There is likewise obviously some plasma stream in the  $x$ -head-ing, along the HFT. Be that as it may, this stream is probably going to be of just auxiliary significance with regards to the rebuilding of the magnetic transition, since it is toward a path generally parallel to the magnetic field, and regardless is not exactly 50 % of the quality of the stream in the  $yz$ -plane (in both pinnacle and normal esteem). Likewise, examination of the structure of  $v_x$  as for the magnetic field lines

demonstrates that in actuality the locales of noteworthy  $v_x$  are found around field lines which don't reconnect.

Closer to the  $x$ -boundary, far from the dissemination region, the stream shows a super position of the stagnation point and shear qualities in steady X-planes. Notwithstanding, the overwhelming plasma stream in the region of the dispersion area is the stagnation point stream. The nearness of a stagnation flow, co-focused with the X-point of  $B_{yz}$ , combined with the nearness of the non-ideal area, is a solid sign that reconnection is happening there. Stagnation point streams are normal for reconnection arrangements and are good for reconnection as they are proficient at localizing physical amounts into little scales (see references in [21]).

We note that the stagnation flow is especially solid in the out-stream headings, comparing to the course along which the current focus is extended. In the solid out stream areas, the plasma velocity comes to over a fourth of the nearby Alfvén speed, whereas in the inflow locales the proportion is regularly not exactly a tenth. This solid outpouring from the reconnection region is driven by the magnetic strain in the recently reconnected field lines. The outpouring “jets” are normal for reconnection, and they are in charge of the circle like spreading of the present fixation at its finishes. This can be seen by examination of the stream and current since the “wings” of the present structure imprint out the districts of the surge jets (see Fig. 4).

One of the real consequences of Hornig and Priest [19] was the disclosure in their unadulterated reconnection arrangement of rotational streams fixated on the X-line, of a contrary sense on either side of the dissemination region. At the point when a perfect stagnation point stream was added to frame the “composite solution”, it was found to overwhelm the stream structure and totally veil the pivot if its quality was over a specific esteem. In spite of the fact that there is no rotational plasma flow evident in our solution, it is as yet conceivable to scan for a foundation turn. So as to do this we look at

$$R = \frac{1}{2\pi R_0} \oint \mathbf{v} dl$$

for closed curve (for this situation we pick circles of radius  $R_0$  in planes of consistent for effortlessness) fixated on the X-line  $x$ -axis). In the event that there is a turn related with the stream in a specific region, at that point this should result in a non-zero estimation of  $R$ . As appeared in Fig. 5, *a*, there is in certainty a turn present in the flow. The turn is for sure observed to be oppositely coordinated on either side of the diffusion region (positive or negative), and has the right sense on each side anticipated by Hornig and Priest [19], concerning the course of the electric current.

In spite of the fact that we expect the shear flow at the  $x$ -boundaries to give a non-zero commitment to, the revolution really increments from the boundaries, inferring that there is some other instrument acting inside the volume to induce the turn. Note additionally that, in the wake of normalizing  $R$  by  $2\pi R_0$ , where  $R_0$  is the span of the way of coordination, we get more grounded pivot nearer to the X-line (truth be told, this isn't carefully the situation). Paradoxically, for round ways of huge range there is basically no additional revolution (over the shear boundary commitment) affected inside the volume, with  $R$  having its maxima at  $x = \pm 0.5$ . This is predictable with the possibility of the pivot tumbling to zero at the boundary of an envelope of room characterized by the

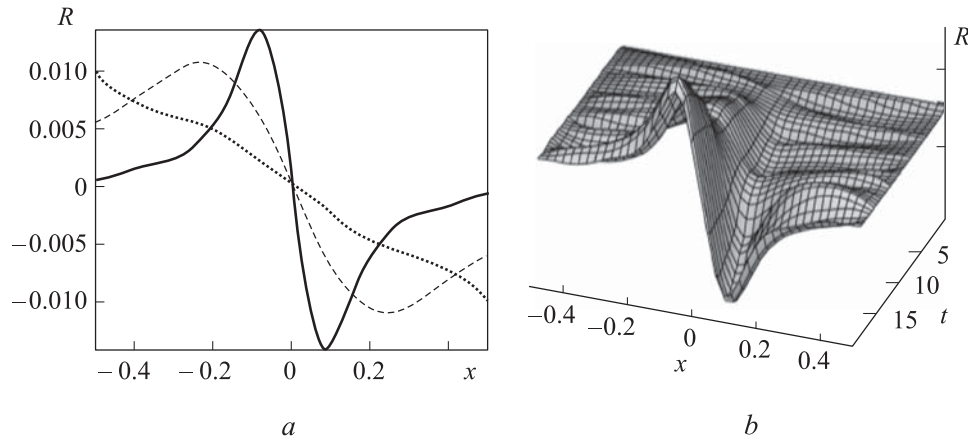


**Fig. 5.** (a) Rotation as a function of  $x$ , calculated for circular circuits of radius 0.01 (solid line), 0.1 (dashed) and 0.2 (dotted), and normalized by  $2\pi R_0$ , where  $R_0$  is the circuit radius. (b) Growth of rotation in time for the circuit of radius 0.01

heap of field lines, which string through the diffusion region, as depicted by Hornig and Priest [19]. Note at long last that the rotational flow develops roughly consistently in time (Fig. 5, *b*), as the current develops. In addition, this development seems to quicken altogether around  $t=12$ , as in the current development, when the reconnection seems to accelerate.

As a trial of this examination, we check the request of size of the foundation turn found. As portrayed by Hornig and Priest [19], the extent of this pivot gives a proportion of the reconnection rate, which may likewise be characterized as  $\int E dl$  a long the X-line. So, assessing

$$\Omega = \frac{1}{2B_x x_0} \int_{y=z=0} E \cdot B dx, \quad (1)$$

where  $B_x$  is the normal magnetic field along the  $x$ -axis inside the diffusion region, and  $x_0$  is the estimated degree of the non-ideal region in the  $x$ -direction, should give roughly similar qualities (to request of extent) as those found for the revolution,  $R$ . A run of the mill estimation of  $\Phi = \int E \cdot B dx$  along the  $x$ -axis is around  $2.5 \cdot 10^{-5}$ , atypical incentive for  $B_x$  is 0.085, and  $x_0$  is roughly 0.1 (at  $x=0.1$ ,  $\eta$  is  $\sim 5\%$  of  $\eta_0$ ). Substituting these qualities into (1) give  $\Omega \approx 0.015$ .

This is in great concurrence with the estimation of the pinnacle revolution as appeared in Fig. 5, *a*.

In summary, even before examining the conduct of the magnetic field lines, as we will go onto do in the pursue area, there is great proof that reconnection is occurring in the focal point of the hyperbolic flux tube. An all-around restricted,

all around settled current focus is available along the HFT axis, in concurrence with the squeezing depicted in Ref. [22] and Ref. [14]. What's more, a stagnation point flow is available in planes in which  $\mathbf{B}$  is hyperbolic, with the stream having solid outpouring locales, which are likewise featured in the present profile by solid wave fronts. Moreover, in the same manner as the aftereffects of Hornig and Priest [19] a foundation turn is observed to be available in the stream, which has inverse sense above and underneath  $D$ , and whose most extreme extent might be intently anticipated by figuring  $\int \mathbf{E} d\mathbf{l}$  along the X-line.

*Field line behavior.* We need to explore the conduct of magnetic field lines which experience the reconnection procedure, and specifically to research the statement of Priest et al. [6] that field lines ceaselessly and persistently change their associations all through the non-ideal region due to the non-presence of an extraordinary field line velocity. So as to do this we choose some specific field lines toward the beginning of the recreation which lie in what will end up being the inflow district. That is, we pursue field lines which meet  $x = 0$  the plane in the region of the line  $x = -z$ , and which toward the beginning of the recreation are arranged appropriately a long way from the diffusion region.

It is essential to make sure that we completely depict the development of the picked field lines, and furthermore to make certain that we in reality follow dependably a similar field line. With the goal that this is the situation, we follow field lines from footpoints, which are affected in the ideal flow, where the magnetic flux is solidified into the plasma. This is accomplished by following field lines at every moment in time from their crossing points with the  $x$ -boundaries, where the estimation of the resistivity is incredibly little. We follow each field line from the two limits into the focal point of the area. While they remain completely in the ideal region, the field lines that are followed from every limit are the equivalent, and can be thought of as interesting field lines. Notwithstanding, once non-ideal procedures become significant, and the field lines that are followed out from relating sets of footpoints are never again co-spatial, at that point we can say that the two footpoint shave become contrastingly associated, or that the first field line has experienced reconnection.

The impact of the reconnection procedure on such a lot of field lines is outlined in Fig. 6. The field lines are followed from focuses at customaryinterims around at first roundabout cross-areas on the boundaries (checked dark). While the field lines stay in the ideal region, we see that comparing sets of footpoints remain (around) connected. Note that the edge of the field lines concerning the  $x$ -hub increments as they are advected towards the X-line ( $x$ -axis). This is because of the expanding shearing on the boundaries.

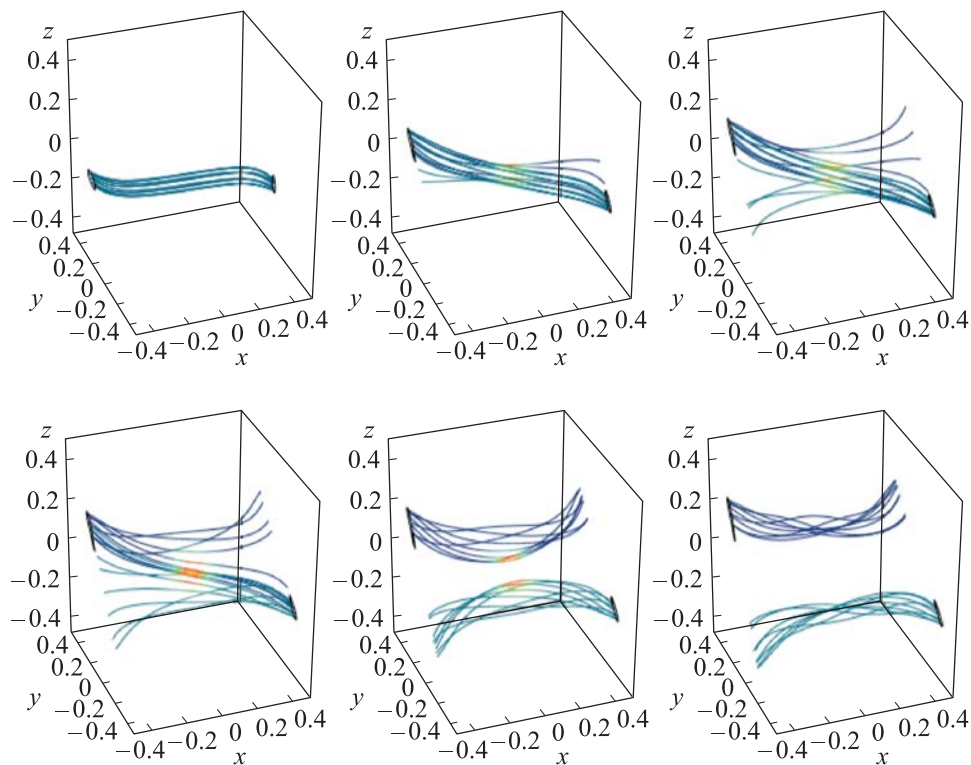


**Fig. 6.** Reconnection of field lines, colored to show the local parallel electric field, with blue being zero and red/yellow being high. The black rings mark the regions from within which field lines are traced on each boundary (Note the change in orientation of these images from that in Fig. 1; the vertical axis is now the  $z$ -rather than  $x$ -direction, so that the imposed flux patches are to left and right of the displayed volume)

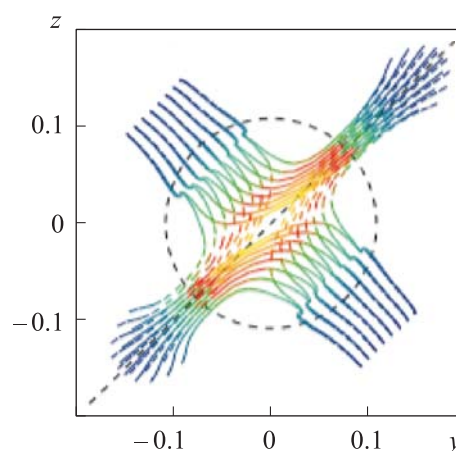
As the magnetic field lines start to enter the non-ideal region (see the second casing in Fig. 6), they begin to change their associations, as field lines followed from at first associated focuses now meet the contrary boundaries a long way from the situation of their inverse footpoints. As they keep on going through the non-ideal locale ( $D$ ), it tends to be seen that the followed field lines flip through the volume, before ending up wherever secured in the perfect stream yet again after they exit  $D$ . This flipping conduct exhibits the persistent reconnection of field lines all through the non-perfect area, since given plasma component (footpoint) in the perfect locale on one side of  $D$  is associated with an alternate plasma component in the ideal region on the opposite side of  $D$  for every moment in time all through the flipping movement. When the field line have completely reconnected (for example passed completely out of non-ideal region once more), we note that the last arrangements of field lines seem turned around

themselves, where initially there was no wind. This shows the nearness of self-helicity inside the plotted arrangements of field lines in the outflow region. This might be gotten by transformation of the underlying helicity of the calculated in stream documented lines on either side of (which are bent and folded over one another because of the limit driving), and furthermore perhaps made by the rotational movement inside the reconnection flow.

The nonstop reconnection of field lines going through the non-ideal region means the distinctive field line speeds for field lines followed from focuses tied down on either side of the non-ideal region. The idea of the befuddling of these two velocities is indicated all the more plainly by plotting the movements of the field line footpoints in a plane which all field lines converge. We pursue the crossing points of sets of field lines  $x = 0$  with the plane for symmetry reasons, in spite of the fact that the image is subjectively the equivalent for other such planes. We indicate the velocity of field lines followed from  $x = -0.5$  as  $w_{in}$ , since this is the course from which magnetic flux goes into  $D$ . Thus, the speed of field lines followed from  $x = 0.5$  is indicated by  $w_{out}$ .

The flow lines of the two speeds,  $w_{in}$  and  $w_{out}$ , for example the ways of the footpoints in the plane, are appeared in Fig. 7. Two arrangements of field lines are followed, this time beginning from two lines of footpoints in the  $x = 0$  plane,

**Fig. 7.** Flow lines of  $w_{in}$  (dashed) and  $w_{out}$  (solid) in the plane  $x = 0$ , colored at each point to show the integrated parallel electric field along the corresponding field line at the corresponding time. The dashed circle shows the radius at which  $\eta \sim 0.05\eta_0$



which are parallel with the long axis (in  $x = 0$ ) of the present focus ( $y = z$ ), and are symmetric about this line. The flow lines of  $w_{in}$  are the dashed lines, while those of  $w_{out}$  are solid.

The flow lines remain around correspondent in the inflow district as the field lines are brought towards the reconnection locale. The slight inconsistency is expected distinctly to the little non-advantageous quality here (due incompletely to numerical impacts) and to numerical mistakes in the field line following. One further unwanted impact which causes additional part of the stream lines is the



kinking which they experience most of the way into wards the beginning. This is because of the Alfvén wave set off by the underlying boundary motion, and had been diminished however much as could be expected, as depicted already. When they achieve the focal district where reconnection is occurring, the flow lines of  $w_{in}$  and  $w_{out}$  veer in all respects unequivocally, and complete the field lines into inverse out stream areas (as can be seen by correlation of Fig. 7 and 4). Inside this focal locale the two arrangements of stream lines normally cross, appearing individual magnetic field lines followed from either side of  $D$  become promptly associated (at the purpose of intersection), before ending up quickly detached once more. In the surge districts, the stream lines, when they have met, remain firmly coordinated once more, showing that the field lines are presently by and by holding their associations.

In synopsis, the crisscrossing of the flow lines of  $w_{in}$  and  $w_{out}$  represents obviously the persistent and consistent reconnection of field lines inside the non-ideal region, and the non-presence of a one of a kind speed portraying the movement of the field lines. The example that we see here is fundamentally the same as that of the “composite arrangement” of Hornig and Priest [19].

## REFERENCES

- [1] Sonnerup B.U.Ö., Paschmann G., Papamastorakis I., et al. Evidence for magnetic field reconnection at the Earth’s magneto pause. *J. Geophys. Res.*, 1981, vol. 86, no. A12, pp. 10049–10067. DOI: <https://doi.org/10.1029/JA086iA12p10049>
- [2] Priest E.R., Lee L.C. Nonlinear magnetic reconnection models with separatrix jets. *J. Plasma Phys.*, 1990, vol. 44, iss. 2, pp. 337–360. DOI: <https://doi.org/10.1017/S0022377800015221>
- [3] Scholer M. Numerical models of magnetic reconnection. *Geophys. Astrophys. Fluid Dyn.*, 1991, vol. 62, iss. 1-4, pp. 51–68. DOI: <https://doi.org/10.1080/03091929108229125>
- [4] Gorbachev V.S. The field topology and frozen-in magnetohydrodynamic flows of plasma in the strong field approximation. PhD thesis. Moscow, Institute of Physics and Engineering, 1998.
- [5] Mandrini C.H., Rovira M.G., Demoulin P., et al. Evidence for magnetic reconnection in large-scale magnetic structures in solar flares. *Astron. Astrophys.*, 1993, vol. 272, pp. 609–620.
- [6] Priest E.R., Hornig G., Pontin D.I. On the nature of three-dimensional magnetic reconnection. *J. Geophys. Res.*, 2003, vol. 108, iss. A7, art. SSH6–1. DOI: <https://doi.org/10.1029/2002JA009812>
- [7] Berger M.A. Three-dimensional reconnection from a global viewpoint. *Proc. Reconnection in Space Plasma*. T. Guyenne, J. Hunt (eds.), vol. SP-285. Paris, ESA, pp. 83–86.

- [8] Schindler K., Hesse M., Birn J. General magnetic reconnection, parallel electric fields, and helicity. *J. Geophys. Res.*, 1988, vol. 93, iss. A6, pp. 5547–5557. DOI: <https://doi.org/10.1029/JA093iA06p05547>
- [9] Hornig G. The geometry of reconnection. In: An introduction to the geometry and topology of fluid flows. Kluwer, 2001, pp. 295–313.
- [10] Yamada M., Ono Y., Hayakawa A., et al. Magnetic reconnection of plasma toroids with cohelicity and counter helicity. *Phys. Rev. Lett.*, 1990, vol. 65, iss. 6, pp. 721–724. DOI: <https://doi.org/10.1103/PhysRevLett.65.721>
- [11] Dahlburg R.B., Antiochos S.K., Norton D. Magnetic flux tube tunneling. *Phys. Rev. E*, 1997, vol. 56, iss. 2, pp. 2094–2103. DOI: <https://doi.org/10.1103/PhysRevE.56.2094>
- [12] Linton M., Dahlburg R.B., Antiochos S.K. Reconnection of twisted flux tubes as a function of contact angle. *Astrophys. J.*, 2001, vol. 553, no. 2, pp. 905–921. DOI: <https://doi.org/10.1086/320974>
- [13] Galsgaard K., Nordlund Å. Heating and activity of the solar corona: 1. Boundary shearing of an initially homogeneous magnetic field. *J. Geophys. Res.*, 1996, vol. 101, iss. A6, pp. 13445–13460. DOI: <https://doi.org/10.1029/96JA00428>
- [14] Galsgaard K., Nordlund Å. Heating and activity of the solar corona: 3. Dynamics of a low beta plasma with 3D null points. *J. Geophys. Res.*, 1997, vol. 102, iss. A1, pp. 231–248. DOI: <https://doi.org/10.1029/96JA02680>
- [15] Milano L.J., Dmitruk P., Mandrini C.H., et al. Quasi-separatrix layers in a reduced magneto hydrodynamic model of a coronal loop. *Astrophys. J.*, 1999, vol. 521, no. 2, pp. 889–897. DOI: <https://doi.org/10.1086/307563>
- [16] Kliem B., Schumacher J. Dynamic three-dimensional spontaneous reconnection in a sheared current sheet. In: Space plasma simulation. Katlenburg-Lindau, Copernicus Gesellschaft, 2001, pp. 264–267.
- [17] Nordlund A., Galsgaard K. A 3D MHD code for parallel computers. Technical report. Astronomical Observatory, Copenhagen Univ., 1997.
- [18] Hyman J.M. A method of lines approach to the numerical solution of conservation laws. In: Advances in computer methods for partial differential equations III. IMACS, 1979, pp. 313–343.
- [19] Hornig G., Priest E.R. Evolution of magnetic flux in an isolated reconnection process. *Phys. Plasmas*, 2003, vol. 10, iss. 7, pp. 2712–1721. DOI: <https://doi.org/10.1063/1.1580120>
- [20] Mellor C., Gerrard C., Galsgaard K., et al. Numerical simulations of the flux tube tectonics model for coronal heating. *Sol. Phys.*, 2005, vol. 227, iss. 1, pp. 39–60. DOI: <https://doi.org/10.1007/s11207-005-1713-2>
- [21] Priest E.R., Forbes T.G. Magnetic reconnection: MHD theory and applications. Cambridge Univ. Press, Cambridge, 2000.


[22] Titov V.S., Galsgaard K., Neukirch T. Magnetic pinching of hyperbolic flux tubes. I. Basic estimations. *Astrophys. J.*, 2003, vol. 582, no. 2, pp. 1172–1189.

DOI: <https://doi.org/10.1086/344799>

**Al-Hachami Ali Khalaf Hussain** — Dr., Department of Mathematics, College of Education for Pure Science, University of Wassit (Al Kūt, Wasit, Iraq).

**Please cite this article as:**

Al-Hachami Ali K.H. Magnetic reconnection in the absence of three-dimension null point. *Herald of the Bauman Moscow State Technical University, Series Natural Sciences*, 2019, no. 6, pp. 50–66. DOI: 10.18698/1812-3368-2019-6-50-66

	<p>В Издательстве МГТУ им. Н.Э. Баумана вышла в свет монография авторов <b>И.В. Фомина, С.В. Червона, А.Н. Морозова</b></p> <p><b>«Гравитационные волны ранней Вселенной»</b></p> <p>Рассмотрены применение скалярных полей в космологии и методы построения моделей ранней Вселенной на основе их динамики. Выполнен анализ динамики Вселенной на различных стадиях ее эволюции. Проведен расчет параметров космологических возмущений. Представлены методы верификации инфляционных моделей и новые методы детектирования гравитационных волн. Для специалистов, интересующихся проблемами нелинейной теории поля, теории гравитации, космологии и гравитационно-волновыми исследованиями, а также студентов старших курсов, магистров и аспирантов.</p> <p><b>По вопросам приобретения обращайтесь:</b> 105005, Москва, 2-я Бауманская ул., д. 5, стр. 1 +7 (499) 263-60-45 <a href="mailto:press@bmstu.ru">press@bmstu.ru</a> <a href="http://baumanpress.ru">http://baumanpress.ru</a></p>
--	---